Title

Near-Quantitative Defluorination of Perfluorinated and Fluorotelomer Carboxylates and Sulfonates with Integrated Oxidation and Reduction.

Journal

Environmental science & technology, 55(10)

ISSN

0013-936X

Authors

Liu, Zekun
Bentel, Michael J
Yu, Yaochun
et al.

Publication Date

2021-05-01

DOI

10.1021/acs.est.1c00353

Environmental Science & Technology

pubs.acs.org/est

Article

Near-Quantitative Defluorination of Perfluorinated and Fluorotelomer Carboxylates and Sulfonates with Integrated Oxidation and Reduction

Zekun Liu,[§] Michael J. Bentel,[§] Yaochun Yu, Changxu Ren, Jinyu Gao, Vivek Francis Pulikkal, Mei Sun, Yujie Men, and Jinyong Liu*

Cite This: https://doi.org/10.1021/acs.est.1c00353

Read Online

ACCESS | Metrics & More | Article Recommendations | Supporting Information

ABSTRACT: The UV-sulfite reductive treatment using hydrated electrons (e_{aq}^-) is a promising technology for destroying perfluorocarboxylates (PFCAs, $C_nF_{2n+1}COO^-$) in any chain length. However, the C−H bonds formed in the transformation products strengthen the residual C−F bonds and thus prevent complete defluorination. Reductive treatments of fluorotelomer carboxylates (FTCAs, $C_nF_{2n+1}-CH_2CH_2-COO^-$) and sulfonates (FTSAs, $C_nF_{2n+1}-CH_2CH_2-SO_3^-$) are also sluggish because the ethylene linker separates the fluoroalkyl chain from the end functional group. In this work, we used oxidation (*Ox*) with hydroxyl radicals (HO•) to convert FTCAs and FTSAs to a mixture of PFCAs. This process also cleaved 35−95% of C−F bonds depending on the fluoroalkyl chain length. We probed the stoichiometry and mechanism for the oxidative defluorination of fluorotelomers. The subsequent reduction (*Red*) with UV-sulfite achieved deep defluorination of the PFCA mixture for up to 90%. The following use of HO• to oxidize the H-rich residues led to the cleavage of the remaining C−F bonds. We examined the efficacy of integrated oxidative and reductive treatment of n = 1−8 PFCAs, n = 4,6,8 perfluorosulfonates (PFSAs, $C_nF_{2n+1}-SO_3^-$), n = 1−8 FTCAs, and n = 4,6,8 FTSAs. A majority of structures yielded near-quantitative overall defluorination (97−103%), except for n = 7,8 fluorotelomers (85−89%), n = 4 PFSA (94%), and n = 4 FTSA (93%). The results show the feasibility of complete defluorination of legacy PFAS pollutants and will advance both remediation technology design and water sample analysis.

KEYWORDS: *defluorination, oxidation, hydroxyl radical, reduction, hydrated electron, perfluorocarboxylate, perfluorosulfonate, fluorotelomer*

INTRODUCTION

Per- and polyfluoroalkyl substances (PFAS) have been developed and used for almost eight decades. The adverse health effects of long-chain PFAS have prompted a phase-out of C8-based chemicals and a shift toward short-chain alternatives.[1−3] A large variety of PFAS with various fluoroalkyl chain lengths and functional groups has been detected in the water environment worldwide.[4−9] Although carbon adsorption, ion exchange, and nanofiltration can rapidly remove PFAS from polluted water,[10−13] the concentrated PFAS in spent sorbents or membrane rejects require cost-effective destruction. Various PFAS destruction technologies have been under rapid development, such as wet oxidation,[14,15] plasma,[16,17] electrochemical,[18−20] photochemical,[21,22] and sonochemical[23,24] approaches. Most technologies utilize strong oxidative species (e.g., hydroxyl radical HO•, sulfate radical SO_4^-•, and semiconductor hole) and/or reductive species (e.g., hydrated electron e_{aq}^-). However, most reports to date have indicated partial defluorination of selected PFAS structures. The fundamental question on the feasibility of complete defluorination (i.e., transforming all C−F bonds into F^- ions) remains.

Under UV irradiation, the e_{aq}^- can be generated from aqueous SO_3^{2-} or other photosensitizers for reductive defluorination.[25−31] In our study on UV-sulfite treatment of perfluorocarboxylates (PFCAs, $C_nF_{2n+1}COO^-$), perfluorosulfonates (PFSAs, $C_nF_{2n+1}-SO_3^-$), and fluorotelomer carboxylates (FTCAs, $C_nF_{2n+1}-CH_2CH_2-COO^-$),[32] PFCAs showed the best degradability and no significant chain-length dependence.[25,26,32] While the favorable defluorination pathway is decarboxylation (i.e., chain-shortening), the e_{aq}^- also converts the most susceptible C−F bonds in the molecule into C−H bonds (i.e., H/F exchange).[32,33] For example, starting from a short-chain PFCA (e.g., $C_3F_7-CF_2-COO^-$), the H/F exchange on the most susceptible α-CF_2 yields $C_3F_7-CH_2-COO^-$. The separation of the short fluoroalkyl chain from

Received: January 17, 2021
Revised: April 7, 2021
Accepted: April 22, 2021

$-COO^-$ caused high recalcitrance against further degradation. Unfortunately, fluorotelomers ($C_nF_{2n+1}-(CH_2)_m-X$) have been the primary PFAS formulation for textiles, carpets, garments, and aqueous film-forming foams (AFFF).[14,34] Therefore, an oxidative pretreatment of fluorotelomers into PFCAs is necessary. However, our recent attempt on UV-sulfite treatment of PFCAs at the optimized pH 12 still could not achieve 100% defluorination.[33] The H/F exchange can significantly strengthen the C−F bonds on neighboring carbons, surpassing the capability of reductive defluorination with e_{aq}^-. In such scenarios, a post-treatment with oxidizing species also seems beneficial to degrade H-rich residues.

Although HO• cannot degrade PFCAs or PFSAs, previous studies have confirmed its efficacy in converting fluorotelomers into PFCAs.[35−37] Interestingly, the treatment of n = 6 FTSA (i.e., 6:2 FTS) with HO• from either heat-activated persulfate or cobalt-activated peroxymonosulfate yielded a mixture of all PFCAs from n = 6 PFHpA to n = 1 TFA. The chain-shortened PFCA products indicate a continuous loss of CF_2 units and thus defluorination, but the mechanism of HO• triggered defluorination has remained elusive. Moreover, oxidants were usually added in great excess (e.g., 1−60 mM $K_2S_2O_8$ or 0.1−100 mM $KHSO_5$) to treat nM to μM levels of fluorotelomers.[35−37] In this study, we optimized and elucidated the oxidative process (*Ox*) using HO• (generated from heat-activation of persulfate under alkaline conditions for a proof-of-concept investigation) and integrated it with the UV-sulfite reductive process (*Red*) to achieve near-quantitative defluorination of a majority of FTCAs, FTSAs, PFCAs, and PFSAs. These results will fill major knowledge gaps in the mechanistic understanding toward thorough PFAS destruction while advancing PFAS remediation technologies and water sample analysis.

MATERIALS AND METHODS

Nomenclature and Definition. To facilitate mechanistic discussion, we refer to all PFAS structures using the number of fluorinated carbons (i.e., the "n" in C_nF_{2n+1}) rather than the total number of carbons in the molecule (i.e., C_n). The latter may generate distraction or confusion (e.g., C_7 PFCA for $C_6F_{13}-COO^-$, C_6 PFSA for $C_6F_{13}-SO_3^-$, and C_9 FTCA for $C_6F_{13}-CH_2CH_2-COO^-$). We also minimize the use of common names because PFHpA, PFHxS, 6:3 FTCA, and 6:2 FTSA share the same $C_6F_{13}-$ moiety. In this paper, the term *degradation* refers to the disappearance of parent compounds upon any structural transformation. The term *destruction* refers specifically to molecular decomposition through the cleavage of C−F bonds via any pathway.

Chemicals. PFCAs (n = 1−8 $C_nF_{2n+1}COO^-$), PFSAs (n = 4,6,8 $C_nF_{2n+1}SO_3^-$), FTCAs (n = 1−8 $C_nF_{2n+1}-CH_2CH_2-COO^-$), and FTSAs (n = 4,6,8 $C_nF_{2n+1}-CH_2CH_2-SO_3^-$) were purchased in bulk quantities (i.e., 0.25−5 g) and used as received. The information on CAS numbers, purities, and vendors are collected in the Supporting Information (SI). The ≥95% purity for all PFAS reagents ensures the measured 85−100% defluorination percentages reflect the reactivity of the labeled chemical rather than that of minor isomers or impurities. Sodium sulfite (Na_2SO_3), potassium persulfate ($K_2S_2O_8$), sulfuric acid (H_2SO_4), sodium hydroxide (NaOH), and sodium bicarbonate ($NaHCO_3$) were purchased from Fisher Chemical.

Experimental Procedures for Fluorotelomer Destruction. *Step 1: Preoxidation.* A 30 mL solution containing 0.5 mM of individual FTCA/FTSA and variable concentrations of $K_2S_2O_8$ was loaded in a 35 mL heavy-wall glass pressure vessel (Synthware Glass). To compare the oxidation products by SO_4^-• and HO•, we adjusted the initial solution pH to 2.0 with H_2SO_4 or to 12.0 (or higher) with NaOH, respectively. At pH ≤ 2, the SO_4^-• from $S_2O_8^{2-}$ homolysis is the dominant oxidative species.[38] At pH ≥ 12, most SO_4^-• reacts with HO^- to yield HO• and SO_4^{2-}.[38] The ratio of $[K_2S_2O_8]$:[fluorotelomer] as low as 10:1 resulted in significant defluorination, and the previously used $[NaOH]:[K_2S_2O_8]$ at 2.5:1[35] could not provide sufficient HO^- to neutralize the HF product and maintain the alkaline pH. Thus, we elevated the $[NaOH]:[K_2S_2O_8]$ ratio to 5:1, which ensured pH ≥ 12 throughout the oxidation. The pressure vessels were loosely capped to avoid pressure build-up, immersed in water inside a 250 mL glass beaker, and transferred into a pressure cooker (Farberware 6 Quart) loaded with 1 L water. The cooker was heated to 120 °C within 20 min and maintained at 120 °C for 40 min. The pressure was then released and the vessels were cooled down on the bench before analysis. Ion chromatography (IC) analysis suggested that all $S_2O_8^{2-}$ were decomposed into two equivalents of sulfate ions (SO_4^{2-}). Under alkaline conditions, excess $S_2O_8^{2-}$ was decomposed into O_2.[39] Therefore, there was little residual $S_2O_8^{2-}$ to impact the following UV/sulfite treatment step.

Step 2: Reduction of Oxidized Products. The resulting solution from Step 1 (30 mL) was diluted into 600 mL so that the new solution represented 0.025 mM of the initial fluorotelomer. This 20x dilution was conducted to ensure an effective reductive treatment of PFCA products. The solution was amended with 10 mM of Na_2SO_3 and 5 mM of $NaHCO_3$, and the pH was adjusted to 12.0 with NaOH. The solution was treated in a closed photochemical reactor with an 18 W low-pressure mercury UV lamp at 20 °C for 4 h. The reactor configuration has been fully described in our previous report (Open Access).[32] The ending pH after the treatment was 11.7−11.9. The treated solution was stirred under air for 24 h to ensure complete oxidation of all residual SO_3^{2-}.[40]

Step 3: Postoxidation. A 29 mL aliquot of the resulting solution from Step 2 was amended with 12.5 mM NaOH and 5 mM $K_2S_2O_8$ (the 2.5 equiv of HO^- were sufficient for this step), and the final volume was adjusted to 30 mL. The solution was treated with the same procedure as used in Step 1.

Experimental Procedures for PFCA and PFSA Destruction. Because oxidation of PFCA/PFSA with HO• is ineffective, 0.025 mM of individual PFCA/PFSA was directly treated with the procedure of Step 2 described above. The reaction time for all PFCAs was 8 h to maximize the reductive defluorination.[33] The reaction time for the three PFSAs was 24 h. Due to the recalcitrance of short-chain PFSAs and first-order decay of sulfite during the reaction,[33] one spike of 10 mM Na_2SO_3 was added at 8 h to sustain the degradation of n = 6 PFHxS, and two spikes of 10 mM Na_2SO_3 were added at 8 and 16 h, respectively, for n = 4 PFBS. The postoxidation followed the procedure of Step 3 described above.

Sample Analyses. The released F^- ion was primarily quantified by an ion-selective electrode (ISE, Fisherbrand accumet solid-state) connected to a Thermo Scientific Orion Versa Star Pro meter. The accuracy of F^- measurement by the ISE was validated by (1) IC[32] and (2) spiking various concentrations of NaF into the solution matrices of *Ox*, *Ox*−*Red*, and *Ox*−*Red*−*Ox* treatment (errors of measurement are all less than ±2.5%, Table S1). The defluorination percentage

https://doi.org/10.1021/acs.est.1c00353
Environ. Sci. Technol. XXXX, XXX, XXX−XXX

Table 1. Defluorination Percentage of All PFAS by UV-Sulfite at pH 9.5 and pH 12.[a]

	FTCA $C_nF_{2n+1}CH_2CH_2COO^-$		FTSA $C_nF_{2n+1}CH_2CH_2SO_3^-$		PFCA $C_nF_{2n+1}COO^-$[b]		PFSA $C_nF_{2n+1}SO_3^-$	
C_nF_{2n+1} length (n)	pH 9.5 (24 h)	pH 12.0 (24 h)	pH 9.5 (24 h)	pH 12.0 (24 h)	pH 9.5 (24 h)	pH 12.0 (8 h)[c]	pH 9.5 (24 h)	pH 12.0 (8 h)[d]
1	0.7 ± 0.1	11.9 ± 0.7			94.1 ± 4.1	100 ± 2.0		
2	0.9 ± 0.2	11.4 ± 3.1			54.2 ± 6.3	72.9 ± 2.0		
3	1.1 ± 0.1	11.1 ± 2.0			48.1 ± 5.2	92.2 ± 2.8		
4	0.7 ± 0.2	11.3 ± 2.2	0.26 ± 0.02	17.8 ± 0.7	50.7 ± 2.7	78.7 ± 7.7	1.5 ± 0.1	32.4 ± 0.2
5	4.1 ± 0.2	27.5 ± 0.8			48.7 ± 6.4	89.3 ± 2.4		
6	7.4 ± 1.8	40.8 ± 1.0	13.2 ± 0.9	68.7 ± 1.1	48.7 ± 2.9	83.4 ± 0.8	18.3 ± 0.9	53.4 ± 2.3
7	12.7 ± 2.1	67.7 ± 0.9			52.3 ± 5.6	93.0 ± 1.6		
8	26.0 ± 2.7	76.0 ± 1.0	34.7 ± 1.1	75.7 ± 1.3	52.2 ± 1.8	81.7 ± 0.0	30.4 ± 0.9	80.1 ± 1.9

[a]Reaction conditions: individual PFAS (0.025 mM), Na_2SO_3 (10 mM), $NaHCO_3$ (5 mM), 254 nm irradiation (18 W low-pressure Hg lamp for a 600 mL solution) at 20 °C. Errors indicate standard deviation of triplicate reactions. [b]Reported in our previous study.[33] [c]Defluorination of all PFCAs reached the maximum within 8 h. [d]Defluorination of n = 8 PFOS reached the maximum within 8 h, while the defluorination of n = 6 PFHxS and n = 4 PFBS required additional spikes of 10 mM Na_2SO_3 to continue efficiently (see Figure 5).

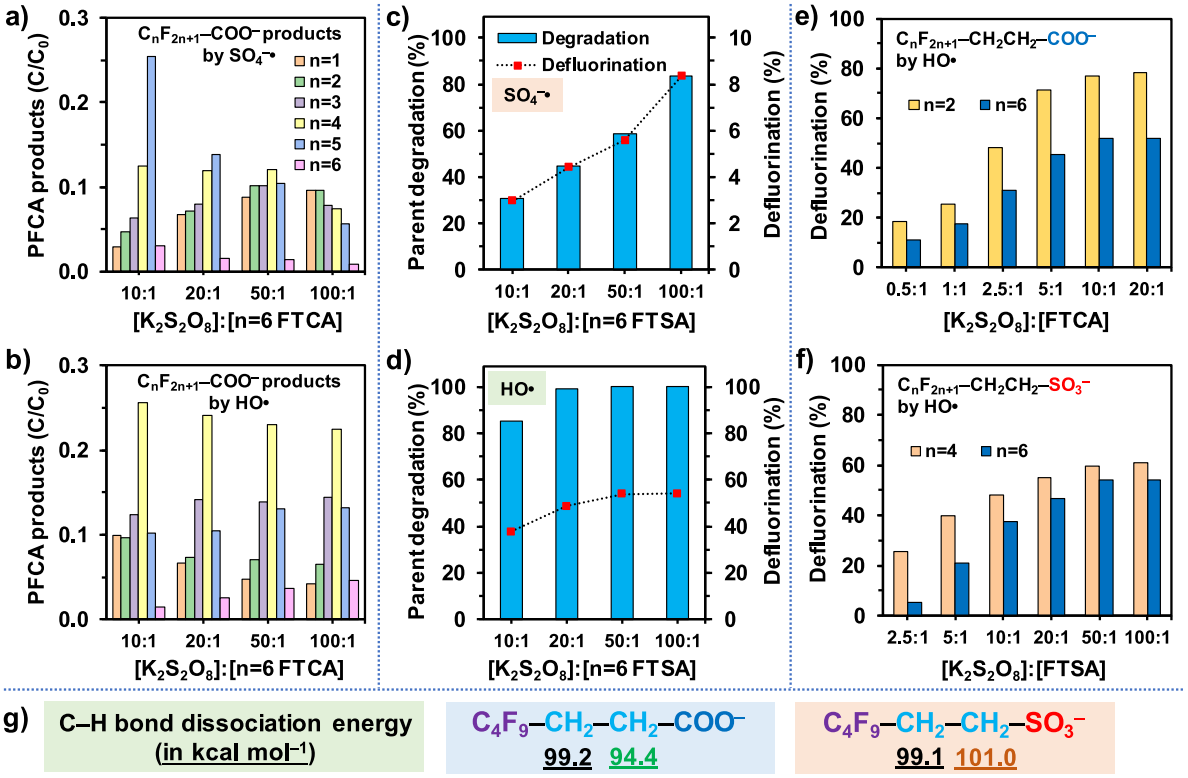

Figure 1. Perfluorocarboxylate (PFCA) products from the oxidative degradation of n = 6 FTCA with (a) SO_4^{-}• and (b) HO•; the percentages of parent degradation and defluorination of n = 6 FTSA with (c) SO_4^{-}• and (d) HO•; the defluorination percentages of (e) n = 2 and 6 FTCA and (f) n = 4 and 6 FTSA with HO• using various $K_2S_2O_8$ dosages; and (g) calculated C−H bond dissociation energies in the representative n = 4 FTCA and FTSA at the B3LYP-D3(BJ)/6-311+G(2d,2p) level of theory.[32,54] All reactions were carried out at 120 °C for 40 min with the initial PFAS concentration of 0.5 mM. The generation of SO_4^{-}• and HO• was achieved at pH ≤ 2 and pH ≥ 12, respectively. Note that the deF% in panel c ranges from 0 to 10%.

(deF%) is defined as the concentration ratio between the released F^- ions in solution and the total fluorine in the parent PFAS molecule. All parent compounds and PFCA products (from the oxidative pretreatment of fluorotelomers) were analyzed by liquid chromatography equipped with a high-resolution quadrupole orbitrap mass spectrometer (LC−HRMS/MS) (Q Exactive, Thermo Fisher Scientific). The analyses of n = 1 and n = 2 PFCAs by LC−HRMS/MS and IC[33] gave very similar results. Total organic fluorine in the treated water samples was determined as adsorbable organic fluorine using combustion−ion chromatography. Detailed information on instrument parameters and quality assurance/control are described in the SI.

RESULTS AND DISCUSSION

Rationales for Oxidative Pretreatment of Fluorotelomers. In FTCAs and FTSAs, the fluoroalkyl chain and the end functional groups (−COO^- and − SO_3^-) are separated by the ethylene linker (−CH_2CH_2−). This structural feature leads to much higher recalcitrance than PFCAs under direct UV-sulfite treatment (Table 1). The degradability of fluorotelomers exhibited a strong dependence on the fluoroalkyl chain length. Our previous report on the structure−reactivity

https://doi.org/10.1021/acs.est.1c00353
Environ. Sci. Technol. XXXX, XXX, XXX−XXX

relationship contains detailed information.[32] Although the elevation of pH from 9.5 to 12.0 substantially enhanced the deF% of all fluorotelomers, the low values for short-chain $n \leq 4$ FTCAs and n = 4 FTSA suggest that direct treatment of fluorotelomers with UV-sulfite is not an effective approach.

In PFCAs, the direct link between $C_nF_{2n+1}-$ and $-COO^-$ has a unique advantage for achieving deep defluorination. The decarboxylation triggers the formation of unstable $C_nF_{2n+1}-OH$, which spontaneously loses two F^- ions from the α-carbon and yields the chain-shortened $C_{n-1}F_{2n-1}-COO^-$.[32] The continuous decarboxylation is the desirable degradation pathway to achieve deep defluorination of PFCAs.[33] The $-COO^-$ also significantly weakens the C−F bond of the α-CF_2 moiety regardless of the chain length, thus enabling a fast H/F exchange on the parent compound.[33] In stark comparison, short-chain fluorotelomers only contain relatively strong C−F bonds in the ethylene-segregated fluoroalkyl moiety. This structural feature leads to slow decay and limited defluorination by direct UV-sulfite treatment even at the optimized pH 12. Therefore, a preoxidation is necessary to convert fluorotelomers into PFCAs.

In this proof-of-concept study, we conducted oxidative reactions using heat activation of $K_2S_2O_8$ at 120 °C. This temperature is readily achievable with an autoclave or pressure cooker and allowed rapid completion of reactions with HO• (see results below). Digestions using $K_2S_2O_8$ and NaOH-$K_2S_2O_8$ have been widely adopted for water quality analyses (e.g., organic carbon,[41,42] total nitrogen,[43] and total phosphorus[44−46]) because both SO_4^-• and HO• can mineralize organic carbons. Control experiments without NaOH and $K_2S_2O_8$ at 120 °C showed negligible defluorination (<0.5%) of both FTCAs and FTSAs (Table S2). The addition of 12.5−125 mM NaOH (pH 12.1−13.1) without $K_2S_2O_8$ slightly increased the defluorination to <2%, indicating that HF elimination[47] from $-CF_2-CH_2CH_2-$ to yield $-CF{=}CHCH_2-$ is trivial even at 120 °C.

Efficacy and Efficiency of SO_4^-• and HO• Radicals. We compared SO_4^-• and HO• in the oxidative treatment of both FTCAs and FTSAs. The use of only $K_2S_2O_8$ with an initial pH at 2.0 preserved SO_4^-• as the dominant oxidant. A dose of 5 mM $K_2S_2O_8$ degraded all the 0.5 mM n = 6 FTCA. The oxidation yielded a mixture of n = 1−6 PFCAs (Figure 1a) and 20% defluorination (Table S3). The gradual increase of $[K_2S_2O_8]$:[n = 6 FTCA] from 10:1 to 100:1 (i.e., from 5 to 50 mM $K_2S_2O_8$ versus 0.5 mM n = 6 FTCA) shifted the dominant PFCA product from n = 5 to n = 1 (Figure 1a) and increased the defluorination from 20 to 42% (Table S3). The result was expected because SO_4^-• is capable of degrading PFCAs through decarboxylation (Scheme 1).[48,49] Similar trends for PFCA product distribution and defluorination were also observed from n = 2 FTCA (Table S4). Because the use of $K_2S_2O_8$ at 100:1 at 120 °C could not achieve complete defluorination, we conclude that the oxidative defluorination of PFCAs using SO_4^-• is not an efficient process. In addition, it is worth noting that a frequently cited mechanism requiring the reaction between C_nF_{2n+1}• and O_2[50] originated from a structure-specific reaction between $•CH_2COO^-$ and O_2[51] via replacing H with F and elongating alkyl chains[50,52,53] without experimental evidence.

When we raised the pH over 12 to convert most SO_4^-• into HO•, the oxidative destruction of n = 6 FTCA showed vastly different results. The variation of $[K_2S_2O_8]$:[n = 6 FTCA] between 10:1 to 100:1 yielded very similar profiles of PFCA products (Figure 1b) and a consistent deF% at 50−52% (Table S5). This level of defluorination is higher than those using SO_4^-• (20−42%). The very low $[K_2S_2O_8]$:[n = 6 FTCA] ratio of 10:1 already achieved the maximum defluorination. Our control experiments confirmed negligible reaction between HO• and PFCAs (deF% < 0.5%, Table S6). Therefore, higher $K_2S_2O_8$ doses (thus higher HO• concentrations at pH ≥ 12) could not further advance the conversion.

Scheme 1. Proposed Mechanism for PFCA Defluorination by SO_4^-•

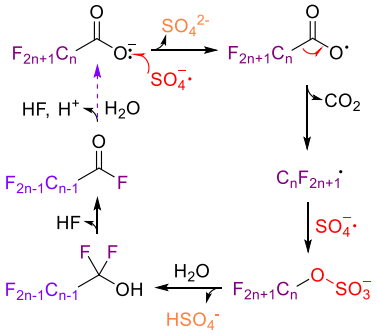

The end functional group of the fluorotelomers also greatly influences the reactivity. The n = 6 FTSA showed much higher recalcitrance than n = 6 FTCA. While ten equivalents of $K_2S_2O_8$ afforded complete degradation of n = 6 FTCA by either SO_4^-• or HO•, the same condition for SO_4^-• oxidation of n = 6 FTSA only achieved 31% degradation and 3.0% defluorination (Figure 1c). Further elevation of $[K_2S_2O_8]$:[n = 6 FTSA] to 100:1 increased the degradation to 83% and the deF% to 8.3%. It seems that each degraded n = 6 FTSA molecule allowed a limited defluorination for 10%. For comparison, the HO• oxidation with $[K_2S_2O_8]$:[n = 6 FTSA] at 10:1 achieved 85% of degradation and 38% of defluorination (Figure 1d). In a recent study, the calculated rate constants for H-abstraction from C−H bonds by HO• is 4 to 8 orders-of-magnitude higher than those by SO_4^-•.[37] Therefore, the poor performance of SO_4^-• oxidation is primarily attributed to the slow kinetics.

We further optimized the $K_2S_2O_8$ dosage for HO• oxidation. For both n = 2 and n = 6 FTCAs, $[K_2S_2O_8]$:[FTCA] at 10:1 was sufficient to maximize defluorination (Figure 1e). For comparison, both n = 4 and n = 6 FTSAs required $[K_2S_2O_8]$:[FTSA]>20:1 to maximize defluorination (Figure 1f). Figure 1d suggests that inadequate defluorination is attributed to the incomplete degradation of the parent compound. We used the established method[32] to calculate bond dissociation energies (BDEs) of C−H bonds in the representative n = 4 FTCA and FTSA (Figure 1g). The weaker α C−H bond in the FTCA explains its higher reactivity than the FTSA, at least in the first step between the parent structure and HO•. In summary, HO• is much more efficient than SO_4^-• for fluorotelomer degradation due to kinetic factors, and FTCAs are more susceptible than FTSAs.

Defluorination and Products from HO• Oxidation. The use of HO• cleaved significant portions of C−F bonds from various FTCAs and FTSAs (Figures 2a). With the optimized $[K_2S_2O_8]$:[FTCA] at 10:1, the deF% of FTCAs increased from 35% to 95% when the fluoroalkyl chain length decreased from n = 8 to n = 1. With the optimized $[K_2S_2O_8]$:[FTSA] at 50:1, the deF% of FTSAs increased from 23% (n = 8) to 59% (n = 4). The two-CF_2-shortened (i.e., n−2) PFCA

https://doi.org/10.1021/acs.est.1c00353
Environ. Sci. Technol. XXXX, XXX, XXX−XXX

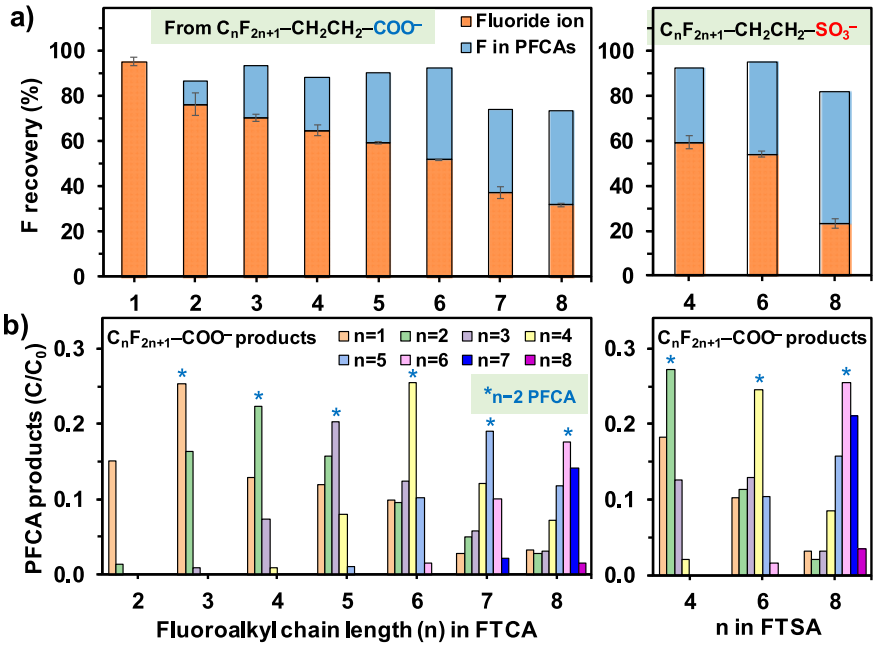

Figure 2. (a) Fluorine balance contributed by F^- ion and total PFCA products and (b) the speciation of individual PFCAs after the HO• oxidation of n = 1−8 FTCAs and n = 4,6,8 FTSAs. The asterisks denote the n−2 PFCA products. Reaction conditions: C_0 = 0.5 mM for individual telomers, $[K_2S_2O_8]$:[FTCA] = 10:1 and $[K_2S_2O_8]$:[FTSA] = 50:1, [NaOH]:$[K_2S_2O_8]$ = 5:1, 120 °C, 40 min.

Scheme 2. Proposed Mechanisms for the Generation of PFCAs in All Chain Lengths from Fluorotelomers

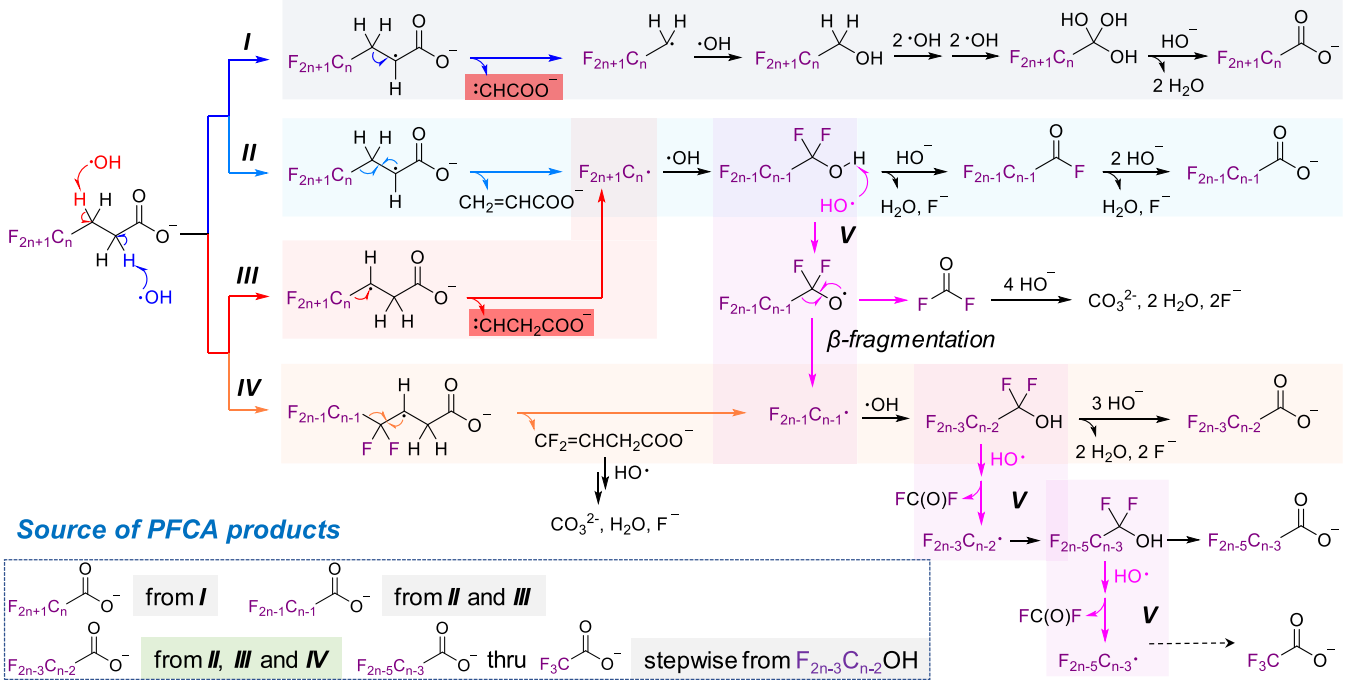

dominated in the product mixtures from all FTCAs and FTSAs (Figures 2b). This observation is consistent with previous studies on total oxidizable precursor (TOP) analysis,[35,55] where diluted fluorotelomers (e.g., 5−60 μg L^{-1}) were treated by more than five orders-of-magnitude higher concentrations of $K_2S_2O_8$ (e.g., 5−60 mM) and 2.5 equiv of NaOH at 85 °C.

For $n \leq 6$ FTCAs and FTSAs, the sum of F^- ion and C−F bonds in the PFCA products recovered 87−95% of the total F balance (Figure 2a). For n = 7,8 FTCA and n = 8 FTSA, the F recovery was relatively low (73−82%). An obvious drop of deF% values was also observed from the three long-chain fluorotelomers. The missing F balance suggests that novel reaction pathways exist, but they primarily transform the hydrocarbon moieties without defluorination. For example, in a recent study on cobalt-activated peroxymonosulfate oxidation of n = 6 FTSA,[37] novel products such as pyruvate (e.g., C_6F_{13}−CO−COO^-) and hydroxylated structures (e.g., C_6F_{13}−$C(OH)_2$−COO^-) were detected. We initially postulated that the low solubility of long-chain fluorotelomers might have been the cause, but lowering the concentration of fluoro-

https://doi.org/10.1021/acs.est.1c00353
Environ. Sci. Technol. XXXX, XXX, XXX−XXX

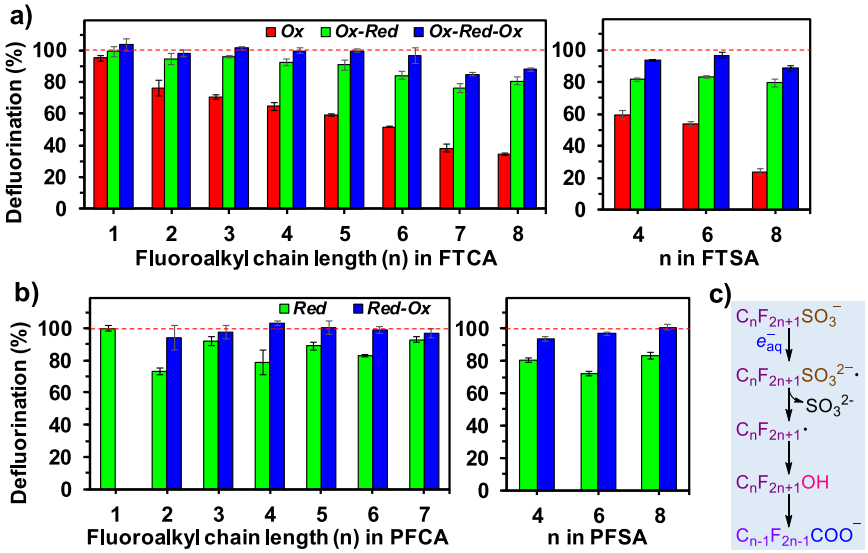

Figure 3. Defluorination from (a) FTCA and FTSA using oxidative pretreatment, UV-sulfite reductive treatment, and oxidative post-treatment (*Ox-Red-Ox*) and from (b) PFCA and PFSA using *Red-Ox*; (c) the reductive conversion of PFSA into PFCA with one CF_2 shortened.

telomers five times did not enhance the deF%. The reason for the different preferences on reaction pathways by short- and long-chain fluorotelomers remains elusive.

Because the majority of F balance is contributed by PFCAs and F^- ions after the HO• oxidation, we propose a set of mechanisms to explain the generation of PFCAs in all chain lengths and the dominance of n−2 PFCA (Scheme 2). After the H abstraction on the α-position CH_2, there are two possible pathways for homolytic C−C bond cleavage. Pathway I yields $C_nF_{2n+1}-CH_2$•, which further reacts with one HO• to form $C_nF_{2n+1}-CH_2OH$. This alcohol can further react with four HO• (two for H abstraction and two for alcohol formation) to yield $C_nF_{2n+1}-C(OH)_3$, which is equivalent to $C_nF_{2n+1}-COOH + H_2O$. However, the C−C bond cleavage requires the single electron to migrate toward the negatively charged carboxylate and possibly generates $:CH-COO^-$. Such an electron migration route is unfavorable. We note that the small product is not necessarily a carbene because one or more HO• may be added during the C−C cleavage to yield $•CH(OH)-COO^-$ or $CH(OH)_2-COO^-$, which are subject to further degradation. Nevertheless, pathway I is less favorable than pathway II, which directly yields C_nF_{2n+1}• and a stable $H_2C=CH-COO^-$. The combination between C_nF_{2n+1}• and HO• yields $C_nF_{2n+1}OH$, which spontaneously decomposes into $C_{n-1}F_{2n-1}COO^-$ (n−1 PFCA) accompanied by the release of two F^- ions.

Following the same rationale, if the initial H abstraction occurs on the β-position CH_2, the less favorable pathway III yields C_nF_{2n+1}•. The more favorable pathway IV directly yields $C_{n-1}F_{2n-1}$• and $F_2C=CH-CH_2-COO^-$. Since unsaturated structures are highly reactive to HO•, a complete defluorination from the latter product can be expected. The further reaction between $C_{n-1}F_{2n-1}$• and HO• yields $C_{n-2}F_{2n-3}COO^-$ (n−2 PFCA) and two F^- ions.

Since HO• cannot react with any PFCA, the formation of n−3 through n = 1 PFCAs may allow H abstraction from perfluorinated alcohol intermediates (pathway V). The radical-involved β-fragmentation shortens the fluoroalkyl chain and yields one $F_2C=O$, which further hydrolyzes into two F^- ions and CO_3^{2-} at pH > 12. Hence, a perfluorinated alcohol ($C_nF_{2n+1}OH$) has two degradation routes. First, HF elimination and hydrolysis yield $C_{n-1}F_{2n-1}COO^-$ as the end product. Second, H abstraction by HO• yields the fluoroalkoxy radical $C_nF_{2n+1}O$•, and the following β-fragmentation will shorten the fluoroalkyl chain to $C_{n-1}F_{2n-1}$•. This mechanism was first proposed by atmospheric chemistry studies[56] and has been adopted to explain electrochemical[18,57] and SO_4^-• oxidation of aqueous PFAS.[58] Further reaction with HO• yields $C_{n-1}F_{2n-1}OH$, which can also follow either of the two routes so that PFCAs in all chain lengths are generated. The n−2 PFCA is generated from two favorable pathways IV and II (followed by pathway V), and its precursor $C_{n-1}F_{2n-1}OH$ is the source of all shorter-chain PFCAs. This explains its dominance in the product mixture from HO• oxidation.

Starting from the parent fluorotelomer, if the degradation reaction stops at any PFCA, two HO• are involved to convert each α-CF_2 into two F^- ions (e.g., pathways II−IV). If pathway V occurs, a third HO• is necessary to enable β-fragmentation, but the resulting fluoroalkyl radical needs another HO• to finish the reaction. This process involves a total of four HO• to defluorinate two CF_2 units (i.e., one HO• for each C−F bond). Thus, a complete defluorination of all C−F bonds from $CF_3-(CF_2)_{n-1}-CH_2CH_2-COO^-$ requires 2n of HO•. The terminal CF_3- will release all three F^- ions via CF_3OH. From another perspective, the oxidation states of C in $-CF_3$, $-CF_2-$, $-CH_2-$ and $-COO^-$ are +3, +2, −2, and +3, respectively. Therefore, regardless of mechanistic details, in order to fully mineralize the FTCA into F^- and CO_2 (or CO_3^{2-} in the alkaline solution), a total of $1 + 2 \times (n-1)+6 \times 2+1 = 2n+12$ of HO• are required. The theoretical stoichiometry between HO• and n = 1−8 FTCAs ranges from 14:1 to 28:1. The corresponding ratios for $[K_2S_2O_8]$:[FTCA] thus range from 7:1 to 14:1. Because the conversion of $C_nF_{2n+1}OH$ into $C_{n-1}F_{2n-1}COO^-$ cannot be mitigated so that the defluorination cannot be 100%, the actual HO• consumption is lower than the theoretical values. The experimentally optimized ratio of $[K_2S_2O_8]$:[FTCA] (Figure 1e) agrees with the theoretical stoichiometry. Therefore, the oxidative treatment of FTCA with $K_2S_2O_8$ + NaOH at 120 °C is highly efficient.

https://doi.org/10.1021/acs.est.1c00353
Environ. Sci. Technol. XXXX, XXX, XXX−XXX

For FTSAs, since the oxidation state of sulfonate S is +5 and will be oxidized to +6 in SO_4^{2-}, the complete mineralization of $C_nF_{2n+1}-CH_2CH_2-SO_3^-$ also requires the same amount of HO• as for FTCAs. The higher amount of HO• required for FTSA than FTCA (Figure 1f) can be attributed to the more recalcitrant α C−H bond (Figure 1g) or other kinetic factors. Nevertheless, the [oxidant]:[substrate] ratio for all fluorotelomers are orders of magnitude lower than those used in previous studies, where a lower reaction temperature or a different persulfate activation mechanism[37] was involved.

Treatment of Fluorotelomer Oxidation Residues and Perfluorinated Acids with UV-Sulfite. To further destroy the PFCA-dominant residues from fluorotelomer preoxidation, we applied UV-sulfite treatment at the optimized pH 12.[33] As expected, significant amounts of F^- ions were released, and the overall deF% reached 76−96% after 8 h (Figures 3a). The deF % of individual PFCAs under the same reaction condition reached 73−93% (Figure 3b). We have elucidated that the incomplete defluorination could be attributed to the H/F exchange reaction[33]

$$C-F + 2e_{aq}^- + H_2O \rightarrow C-H + F^- + OH^-$$

We calculated C−F BDEs on the n = 4 PFCA backbone during the theoretical stepwise reactions by assuming that the H/F exchange occurs at the weakest C−F bond of each possible intermediate without chain-shortening (Figure 4). If the carbon backbone remains intact, the H/F exchange reactions significantly increase the recalcitrance of remaining C−F bonds. The e_{aq}^- cannot directly cleave strong C−F bonds (i.e., BDE > 120 kcal mol^{-1}) even at the optimized reaction condition.[33]

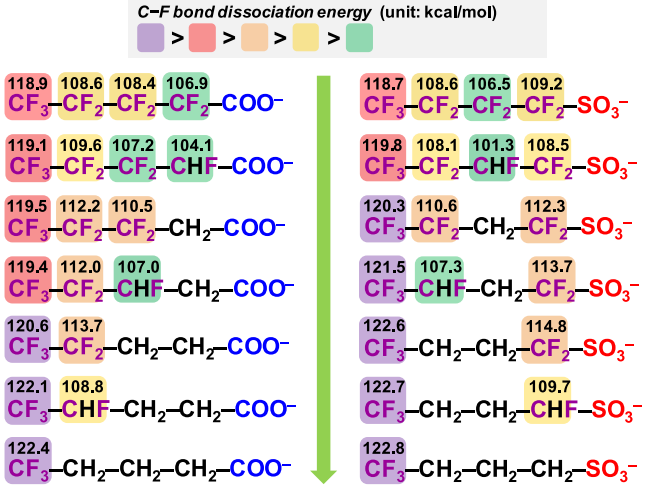

Figure 4. Change of calculated C−F BDEs at the B3LYP-D3(BJ)/6-311+G(2d,2p) level of theory for H/F exchange intermediates from *n* = 4 PFCA and PFSA without chain-shortening. Note that only the weakest C−F bond is replaced by C−H at each step; other intermediate structures and pathways are also possible.

At pH 12, the degradation and defluorination of PFSAs were also significantly enhanced than the previously tested pH 9.5 (Table 2).[32] Under UV-sulfite treatment, PFSAs were much more recalcitrant than PFCAs and showed a strong chain-length dependence (Table 1).[26,32] After 8 h, the degradation of n = 8 PFOS was complete, while the degradation of parent n = 6 PFHxS and n = 4 PFBS were 71% and 34%, respectively (Figure 5a). Because >75% of the initially added 10 mM of sulfite had been depleted after 8 h,[33] we spiked another 10 mM of Na_2SO_3 to support further degradation. After 16 h, the accumulative degradation of PFHxS and PFBS reached 99% and 70%, respectively. Another spike of 10 mM of Na_2SO_3 continued the degradation of PFBS for a total of 86% after 24 h. The three PFSAs allowed the deF% at 84% for PFOS, 72% for PFHxS, and 69% for PFBS after 24 h (Figure 5b). Because there was still 14% of parent compound remaining, the deF% of the degraded portion of PFBS reached 80%. This ratio is consistent with the PFBS degradation without Na_2SO_3 spikes

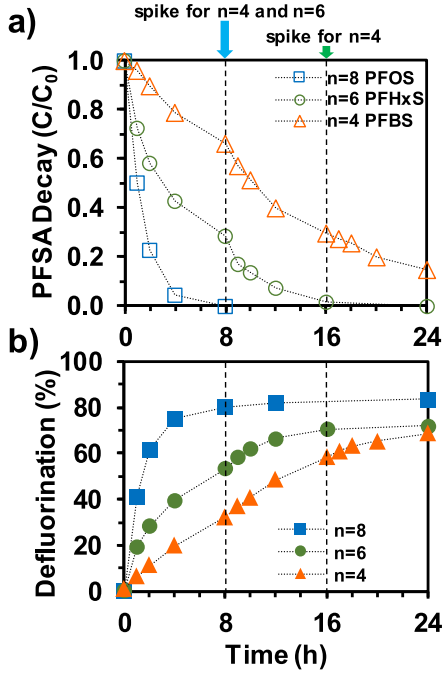

Figure 5. (a) Parent compound degradation (pseudo-first-order fitting shown in Table 2) and (b) defluorination of PFSAs with UV-sulfite treatment. Reaction conditions: 0.025 mM individual PFSA, 10 mM Na_2SO_3, pH 12.0, 254 nm (one 18 W low-pressure mercury lamp for 600 mL of solution), 20 °C. The spikes of 10 mM Na_2SO_3 were added at 8 and 16 h.

Table 2. Degradation of n = 4 and n = 8 PFSAs by UV-Sulfite Treatment at pH 9.5 and 12

	parent degradation		total deF%		molecular deF%[a]		rate constant (h^{-1})[b]	
PFSA ($C_nF_{2n+1}-SO_3^-$)	pH 9.5[c] (48 h)	pH 12 (24 h)	pH 9.5[c] (48 h)	pH 12 (24 h)	pH 9.5[c] (48 h)	pH 12 (24 h)	pH 9.5[c]	pH 12
n = 4 PFBS	6%	52%[d]	4%	41%[d]	67%	79%[d]	0.0013	0.0527
n = 8 PFOS	96%	100%	57%	84%	59%	84%	0.0893	0.7805

[a]The average deF% for the degraded parent compound as (total deF%) divided by (parent degradation). [b]Fit with data within the first 8 h using the pseudo-first-order kinetic model. [c]Data from our previous report.[32] [d]No spikes of 10 mM Na_2SO_3 at 8 and 16 h; this is different from the experiment shown in Figure 5.

https://doi.org/10.1021/acs.est.1c00353
Environ. Sci. Technol. XXXX, XXX, XXX−XXX

(79%, Table 2). Therefore, a relatively high consumption of sulfite is necessary to fully degrade the highly recalcitrant PFBS. However, the degradation intermediates appear to have higher reactivity to reach the limit of ~80% for defluorination. Previous works have identified at least two mechanisms for PFSA destruction. First, the C−S bond cleavage upon reacting with e_{aq}^- converts PFSAs into PFCAs (Figure 3c).[28,32] Second, multiple H/F exchanges on the PFOS backbone without chain-shortening have been observed in our previous study on UV-sulfite treatment at pH 9.5.[32] We calculated C−F BDEs for n = 4 PFSA and possible reaction intermediates (Figure 4) and observed similar trends to those for n = 4 PFCA. On the basis of the knowledge acquired from fluorotelomer preoxidation, the residual C−F bonds in the H-rich residues must be cleaved via a similar oxidative mechanism.

Further Defluorination of UV-Sulfite Treatment Residues with HO• Oxidation. Upon the postoxidation with NaOH-$K_2S_2O_8$ digestion, a majority of structures achieved near-quantitative overall defluorination (97−103%, Figure 3). The additional defluorination in the last step verified that oxidation with HO• is effective in cleaving recalcitrant C−F bonds in the H-rich residues. The most probable mechanism is through the formation of fluorinated alcohols, which spontaneously decompose regardless of the C−F BDE.[32,54] Because a majority of transformation products from UV-sulfite treatment has not been fully characterized,[33] the understanding of detailed mechanisms will need future studies.

The exceptions from near-complete defluorination include n = 7 and 8 FTCA (85% and 88%, respectively) and n = 8 FTSA (89%), as well as n = 4 PFSA (94%) and n = 4 FTSA (93%). Adsorbable organic fluorine analysis on the *Ox-Red-Ox* treated final samples from n = 8 FTCA and FTSA recovered a significant portion of organic fluorine and almost closed the F mass balance (Table S7). Again, the preoxidation of n = 7/8 fluorotelomers released less-than-expected F^- ions and showed relatively large gaps in the F mass balance (Figure 2a). This result suggests other unknown transformation mechanisms that led to non-PFCA products, which were relatively recalcitrant in the following *Red-Ox* treatment.

Implications for PFAS Destruction and Detection. The integration of HO• oxidation and e_{aq}^- reduction achieves deep defluorination of four major legacy PFAS categories- FTCA, FTSA, PFCA, and PFSA. The entire reaction scheme requires only three common chemicals ($K_2S_2O_8$, Na_2SO_3, and NaOH) and two common energy inputs (120 °C heating and 254 nm irradiation). To ensure accurate F^- ion measurement and avoid significant accumulation of SO_4^{2-} from the current experimental settings, we only conducted the *Red-Ox* treatment once. However, as revealed by the results from fluorotelomer oxidation, the reaction between HO• and polyfluorinated structures does not cleave all C−F bonds. It is thus possible that the postoxidation does not necessarily cleave all C−F bonds in the UV-sulfite treatment residues. Further defluorination is possible from repeated *Red-Ox* treatment cycles. Other approaches, such as plasma, electrochemical, and photocatalytic processes, can provide simultaneous or alternating oxidative and reductive conditions. Thus, mechanistic insights obtained from this study are valuable for process design toward the complete destruction of all PFAS structures. For specific water samples, the effects of solution matrices on both *Red* and *Ox* processes also need to be systematically investigated.

Although the treatment of water samples at the ambient temperature is ideal, wet oxidation of PFAS without heating usually requires a high dose of oxidants and long reaction times.[14,15,37,59] The high efficiency of HO• oxidation at 120 °C suggests the value of applying autoclave conditions to rapidly treat specific PFAS wastes with minimal consumption of oxidants. We note that heating the water from 20 to 120 °C requires about 392 kJ kg^{-1} (Text S1). For comparison, the equivalent energy consumption by an 18 W UV lamp for six hours is 389 kJ. As most UV irradiation energy is dissipated as heat, the *Red* process using UV-sulfite or other UV-activated oxidation processes[29,59] can provide the required thermal energy. HO• shows much higher efficiency than SO_4^{-}• in the oxidative destruction of fluorotelomers. Because fluorotelomers and their derived surfactants have become a major category of PFAS pollutants, the use of HO• is highly beneficial to the *Ox-Red-Ox* reaction scheme. Moreover, the pH adjustment in the first *Ox* step serves all three steps that show the highest efficiency under alkaline conditions.

Of notable interest, the very deep defluorination from a majority of PFAS structures also suggests the potential of using the *Ox-Red-Ox* approach to measure total fluorine through the released F^- ion, as long as the total fluorine concentration is above the limit of quantitation by ISE or IC. NaOH-$K_2S_2O_8$ digestion has been widely used to measure total phosphorus (all phosphorus species is converted into orthophosphate for colorimetry or IC analysis) and organic phosphorus (i.e., the difference between the total phosphorus and the orthophosphate without oxidative digestion).[44−46] Similarly, for PFAS analysis, a conceptual analysis kit using $K_2S_2O_8$, Na_2SO_3, NaOH, and a "UV box" to run the *Ox-Red-Ox* sample treatment will enable a simple and inexpensive analysis of "organic fluorine" without mass spectrometry. The mechanistic insights and technical details of this study will benefit the development of such methods. The use of a medium-pressure mercury lamp can further accelerate the UV-mediated *Red* step.[60]

Lastly, since both HO• and e_{aq}^- can be generated in natural aquatic systems,[61−63] we postulate that both poly- and perfluorinated structures are theoretically degradable even if the rate and extent of destruction are very limited. Mechanistic insights of this work may raise research interests to revisit the issue of whether or not PFAS are strictly "forever chemicals" in nature.

■ ASSOCIATED CONTENT

Supporting Information

The Supporting Information is available free of charge at https://pubs.acs.org/doi/10.1021/acs.est.1c00353.

Accuracy of fluoride ion measurement in the treatment solution matrices; the effect of NaOH and $K_2S_2O_8$ on the treatment of FTCAs, FTSAs, and PFCAs; total fluorine analysis results; details of PFAS chemicals; measurement of PFAS parent compounds, transformation products, and total organic fluorine; energy consumption for heat-activated oxidation (PDF)

■ AUTHOR INFORMATION

Corresponding Author

Jinyong Liu − *Department of Chemical & Environmental Engineering, University of California, Riverside, California*

https://doi.org/10.1021/acs.est.1c00353
Environ. Sci. Technol. XXXX, XXX, XXX−XXX

92521, United States; orcid.org/0000-0003-1473-5377; Email: jinyongl@ucr.edu, jinyong.liu101@gmail.com

Authors

Zekun Liu − *Department of Chemical & Environmental Engineering, University of California, Riverside, California 92521, United States;* orcid.org/0000-0003-3802-2662

Michael J. Bentel − *Department of Chemical & Environmental Engineering, University of California, Riverside, California 92521, United States;* orcid.org/0000-0003-1404-113X

Yaochun Yu − *Department of Chemical & Environmental Engineering, University of California, Riverside, California 92521, United States; Department of Civil & Environmental Engineering, University of Illinois at Urbana−Champaign, Urbana, Illinois 61801, United States;* orcid.org/0000-0001-9231-6026

Changxu Ren − *Department of Chemical & Environmental Engineering, University of California, Riverside, California 92521, United States;* orcid.org/0000-0002-1109-794X

Jinyu Gao − *Department of Chemical & Environmental Engineering, University of California, Riverside, California 92521, United States;* orcid.org/0000-0002-1751-3430

Vivek Francis Pulikkal − *Department of Civil & Environmental Engineering, University of North Carolina at Charlotte, Charlotte, North Carolina 28223, United States*

Mei Sun − *Department of Civil & Environmental Engineering, University of North Carolina at Charlotte, Charlotte, North Carolina 28223, United States;* orcid.org/0000-0001-5854-9862

Yujie Men − *Department of Chemical & Environmental Engineering, University of California, Riverside, California 92521, United States; Department of Civil & Environmental Engineering, University of Illinois at Urbana−Champaign, Urbana, Illinois 61801, United States;* orcid.org/0000-0001-9811-3828

Complete contact information is available at: https://pubs.acs.org/10.1021/acs.est.1c00353

Author Contributions

[§]These authors contributed equally.

Notes

The authors declare no competing financial interest.

■ ACKNOWLEDGMENTS

Financial support was provided by the Strategic Environmental Research and Development Program (ER18-1289 for J.L., Z.L., and M.J.B.; ER18-1497 for J.L., M.S., and V.F.P.) and the National Science Foundation (CHE-1709286 for Y.M. and Y.Y.).

■ REFERENCES

(1) Wang, Z.; DeWitt, J. C.; Higgins, C. P.; Cousins, I. T. A never-ending story of per- and polyfluoroalkyl substances (PFASs)? *Environ. Sci. Technol.* **2017**, *51*, 2508−2518.

(2) Ateia, M.; Maroli, A.; Tharayil, N.; Karanfil, T. The overlooked short-and ultrashort-chain poly-and perfluorinated substances: A review. *Chemosphere* **2019**, *220*, 866−882.

(3) Li, F.; Duan, J.; Tian, S.; Ji, H.; Zhu, Y.; Wei, Z.; Zhao, D. Short-chain per-and polyfluoroalkyl substances in aquatic systems: Occurrence, impacts and treatment. *Chem. Eng. J.* **2020**, *380*, 122506.

(4) Schwichtenberg, T.; Bogdan, D.; Carignan, C. C.; Reardon, P.; Rewerts, J.; Wanzek, T.; Field, J. A. PFAS and dissolved organic carbon enrichment in surface water foams on a northern US freshwater lake. *Environ. Sci. Technol.* **2020**, *54*, 14455−14464.

(5) Chen, H.; Munoz, G.; Duy, S. V.; Zhang, L.; Yao, Y.; Zhao, Z.; Yi, L.; Liu, M.; Sun, H.; Liu, J. Occurrence and distribution of per-and polyfluoroalkyl substances in Tianjin, China: The contribution of emerging and unknown analogues. *Environ. Sci. Technol.* **2020**, *54*, 14254−14264.

(6) Zhang, X.; Lohmann, R.; Sunderland, E. M. Poly- and perfluoroalkyl substances in seawater and plankton from the northwestern Atlantic margin. *Environ. Sci. Technol.* **2019**, *53*, 12348−12356.

(7) Chen, H.; Yao, Y.; Zhao, Z.; Wang, Y.; Wang, Q.; Ren, C.; Wang, B.; Sun, H.; Alder, A. C.; Kannan, K. Multimedia distribution and transfer of per-and polyfluoroalkyl substances (PFASs) surrounding two fluorochemical manufacturing facilities in Fuxin, China. *Environ. Sci. Technol.* **2018**, *52*, 8263−8271.

(8) Gebbink, W. A.; van Asseldonk, L.; van Leeuwen, S. P. Presence of emerging per-and polyfluoroalkyl substances (PFASs) in river and drinking water near a fluorochemical production plant in the Netherlands. *Environ. Sci. Technol.* **2017**, *51*, 11057−11065.

(9) D'Agostino, L. A.; Mabury, S. A. Certain perfluoroalkyl and polyfluoroalkyl substances associated with aqueous film forming foam are widespread in Canadian surface waters. *Environ. Sci. Technol.* **2017**, *51*, 13603−13613.

(10) Appleman, T. D.; Higgins, C. P.; Qui'ones, O.; Vanderford, B. J.; Kolstad, C.; Zeigler-Holady, J. C.; Dickenson, E. R. Treatment of poly-and perfluoroalkyl substances in US full-scale water treatment systems. *Water Res.* **2014**, *51*, 246−255.

(11) McCleaf, P.; Englund, S.; Östlund, A.; Lindegren, K.; Wiberg, K.; Ahrens, L. Removal efficiency of multiple poly-and perfluoroalkyl substances (PFASs) in drinking water using granular activated carbon (GAC) and anion exchange (AE) column tests. *Water Res.* **2017**, *120*, 77−87.

(12) Xiao, X.; Ulrich, B. A.; Chen, B.; Higgins, C. P. Sorption of poly- and perfluoroalkyl substances (PFASs) relevant to aqueous film-forming foam (AFFF)-impacted groundwater by biochars and activated carbon. *Environ. Sci. Technol.* **2017**, *51*, 6342−6351.

(13) Steinle-Darling, E.; Reinhard, M. Nanofiltration for trace organic contaminant removal: Structure, solution, and membrane fouling effects on the rejection of perfluorochemicals. *Environ. Sci. Technol.* **2008**, *42*, 5292−5297.

(14) Bruton, T. A.; Sedlak, D. L. Treatment of aqueous film-forming foam by heat-activated persulfate under conditions representative of in situ chemical oxidation. *Environ. Sci. Technol.* **2017**, *51*, 13878−13885.

(15) Park, S.; Lee, L. S.; Medina, V. F.; Zull, A.; Waisner, S. Heat-activated persulfate oxidation of PFOA, 6:2 fluorotelomer sulfonate, and PFOS under conditions suitable for in-situ groundwater remediation. *Chemosphere* **2016**, *145*, 376−383.

(16) Singh, R. K.; Multari, N.; Nau-Hix, C.; Woodard, S.; Nickelsen, M.; Mededovic Thagard, S.; Holsen, T. M. Removal of poly- and perfluorinated compounds from ion exchange regenerant still bottom samples in a plasma reactor. *Environ. Sci. Technol.* **2020**, *54*, 13973−13980.

(17) Saleem, M.; Biondo, O.; Sretenović, G.; Tomei, G.; Magarotto, M.; Pavarin, D.; Marotta, E.; Paradisi, C. Comparative performance assessment of plasma reactors for the treatment of PFOA; Reactor design, kinetics, mineralization and energy yield. *Chem. Eng. J.* **2020**, *382*, 123031.

(18) Radjenovic, J.; Duinslaeger, N.; Avval, S. S.; Chaplin, B. P. Facing the challenge of poly-and perfluoroalkyl substances in water: Is electrochemical oxidation the answer? *Environ. Sci. Technol.* **2020**, *54*, 14815−14829.

(19) Yang, Y. Recent advances in the electrochemical oxidation water treatment: Spotlight on byproduct control. *Front. Environ. Sci. Eng.* **2020**, *14*, 85.

(20) Schaefer, C. E.; Andaya, C.; Urtiaga, A.; McKenzie, E. R.; Higgins, C. P. Electrochemical treatment of perfluorooctanoic acid (PFOA) and perfluorooctane sulfonic acid (PFOS) in groundwater

impacted by aqueous film forming foams (AFFFs). *J. Hazard. Mater.* **2015**, *295*, 170−175.
(21) Qanbarzadeh, M.; Wang, D.; Ateia, M.; Sahu, S. P.; Cates, E. L. Impacts of reactor configuration, degradation mechanisms, and water matrices on perfluorocarboxylic acid treatment efficiency by the UV/$Bi_3O(OH)(PO_4)_2$ photocatalytic process. *ACS ES&T Eng.* **2021**, *1*, 239−248.
(22) Cui, J.; Gao, P.; Deng, Y. Destruction of per- and polyfluoroalkyl substances (PFAS) with advanced reduction processes (ARPs): A critical review. *Environ. Sci. Technol.* **2020**, *54*, 3752−3766.
(23) Moriwaki, H.; Takagi, Y.; Tanaka, M.; Tsuruho, K.; Okitsu, K.; Maeda, Y. Sonochemical decomposition of perfluorooctane sulfonate and perfluorooctanoic acid. *Environ. Sci. Technol.* **2005**, *39*, 3388−3392.
(24) Campbell, T. Y.; Vecitis, C. D.; Mader, B. T.; Hoffmann, M. R. Perfluorinated surfactant chain-length effects on sonochemical kinetics. *J. Phys. Chem. A* **2009**, *113*, 9834−9842.
(25) Huang, L.; Dong, W.; Hou, H. Investigation of the reactivity of hydrated electron toward perfluorinated carboxylates by laser flash photolysis. *Chem. Phys. Lett.* **2007**, *436*, 124−128.
(26) Park, H.; Vecitis, C. D.; Cheng, J.; Choi, W.; Mader, B. T.; Hoffmann, M. R. Reductive defluorination of aqueous perfluorinated alkyl surfactants: Effects of ionic headgroup and chain length. *J. Phys. Chem. A* **2009**, *113*, 690−696.
(27) Song, Z.; Tang, H.; Wang, N.; Zhu, L. Reductive defluorination of perfluorooctanoic acid by hydrated electrons in a sulfite-mediated UV photochemical system. *J. Hazard. Mater.* **2013**, *262*, 332−338.
(28) Tian, H.; Gao, J.; Li, H.; Boyd, S. A.; Gu, C. Complete defluorination of perfluorinated compounds by hydrated electrons generated from 3-indole-acetic-acid in organomodified montmorillonite. *Sci. Rep.* **2016**, *6*, 32949.
(29) Bao, Y.; Deng, S.; Jiang, X.; Qu, Y.; He, Y.; Liu, L.; Chai, Q.; Mumtaz, M.; Huang, J.; Cagnetta, G.; Yu, G. Degradation of PFOA substitute: GenX (HFPO-DA ammonium salt): Oxidation with UV/persulfate or reduction with UV/sulfite? *Environ. Sci. Technol.* **2018**, *52*, 11728−11734.
(30) Sun, Z.; Zhang, C.; Xing, L.; Zhou, Q.; Dong, W.; Hoffmann, M. R. UV/nitrilotriacetic acid process as a novel strategy for efficient photoreductive degradation of perfluorooctanesulfonate. *Environ. Sci. Technol.* **2018**, *52*, 2953−2962.
(31) Chen, Z.; Li, C.; Gao, J.; Dong, H.; Chen, Y.; Wu, B.; Gu, C. Efficient reductive destruction of perfluoroalkyl substances under self-assembled micelle confinement. *Environ. Sci. Technol.* **2020**, *54*, 5178−5185.
(32) Bentel, M. J.; Yu, Y.; Xu, L.; Li, Z.; Wong, B. M.; Men, Y.; Liu, J. Defluorination of per-and polyfluoroalkyl substances (PFASs) with hydrated electrons: Structural dependence and implications to PFAS remediation and management. *Environ. Sci. Technol.* **2019**, *53*, 3718−3728.
(33) Bentel, M. J.; Liu, Z.; Yu, Y.; Gao, J.; Men, Y.; Liu, J. Enhanced degradation of perfluorocarboxylic acids (PFCAs) by UV/sulfite treatment: Reaction mechanisms and system efficiencies at pH 12. *Environ. Sci. Technol. Lett.* **2020**, *7*, 351−357.
(34) Li, L.; Liu, J.; Hu, J.; Wania, F. Degradation of fluorotelomer-based polymers contributes to the global occurrence of fluorotelomer alcohol and perfluoroalkyl carboxylates: A combined dynamic substance flow and environmental fate modeling analysis. *Environ. Sci. Technol.* **2017**, *51*, 4461−4470.
(35) Houtz, E. F.; Sedlak, D. L. Oxidative conversion as a means of detecting precursors to perfluoroalkyl acids in urban runoff. *Environ. Sci. Technol.* **2012**, *46*, 9342−9349.
(36) Zhu, B.; Jiang, W.; Wang, W.; Lin, Y.; Ruan, T.; Jiang, G. Occurrence and degradation potential of fluoroalkylsilane substances as precursors of perfluoroalkyl carboxylic acids. *Environ. Sci. Technol.* **2019**, *53*, 4823−4831.
(37) Zhang, Y.; Liu, J.; Moores, A.; Ghoshal, S. Transformation of 6:2 fluorotelomer sulfonate by cobalt (II)-activated peroxymonosulfate. *Environ. Sci. Technol.* **2020**, *54*, 4631−4640.
(38) Neta, P.; Huie, R. E.; Ross, A. B. Rate constants for reactions of inorganic radicals in aqueous solution. *J. Phys. Chem. Ref. Data* **1988**, *17*, 1027−1284.
(39) Kolthoff, I.; Miller, I. The chemistry of persulfate. I. The kinetics and mechanism of the decomposition of the persulfate ion in aqueous medium1. *J. Am. Chem. Soc.* **1951**, *73*, 3055−3059.
(40) Fuller, E. C.; Crist, R. The rate of oxidation of sulfite ions by oxygen. *J. Am. Chem. Soc.* **1941**, *63*, 1644−1650.
(41) Wilson, R. F. Measure of organic carbon in seawater. *Limnol. Oceanogr.* **1961**, *6*, 259−261.
(42) Menzel, D. W.; Vaccaro, R. F. The measurement of dissolved organic and particulate carbon in seawater. *Limnol. Oceanogr.* **1964**, *9*, 138−142.
(43) Hosomi, M.; Sudo, R. Simultaneous determination of total nitrogen and total phosphorus in freshwater samples using persulfate digestion. *Int. J. Environ. Stud.* **1986**, *27*, 267−275.
(44) Menzel, D. W.; Corwin, N. The measurement of total phosphorus in seawater based on the liberation of organically bound fractions by persulfate oxidation. *Limnol. Oceanogr.* **1965**, *10*, 280−282.
(45) Liu, J.; Wang, H.; Yang, H.; Ma, Y.; Cai, O. Detection of phosphorus species in sediments of artificial landscape lakes in China by fractionation and phosphorus-31 nuclear magnetic resonance spectroscopy. *Environ. Pollut.* **2009**, *157*, 49−56.
(46) Cai, O.; Xiong, Y.; Yang, H.; Liu, J.; Wang, H. Phosphorus transformation under the influence of aluminum, organic carbon, and dissolved oxygen at the water-sediment interface: A simulative study. *Front. Environ. Sci. Eng.* **2020**, *14*, 50.
(47) Phillips, M. M.; Dinglasan-Panlilio, M. J. A.; Mabury, S. A.; Solomon, K. R.; Sibley, P. K. Fluorotelomer acids are more toxic than perfluorinated acids. *Environ. Sci. Technol.* **2007**, *41*, 7159−7163.
(48) Hori, H.; Yamamoto, A.; Hayakawa, E.; Taniyasu, S.; Yamashita, N.; Kutsuna, S.; Kiatagawa, H.; Arakawa, R. Efficient decomposition of environmentally persistent perfluorocarboxylic acids by use of persulfate as a photochemical oxidant. *Environ. Sci. Technol.* **2005**, *39*, 2383−2388.
(49) Liu, C.; Higgins, C.; Wang, F.; Shih, K. Effect of temperature on oxidative transformation of perfluorooctanoic acid (PFOA) by persulfate activation in water. *Sep. Purif. Technol.* **2012**, *91*, 46−51.
(50) Vecitis, C. D.; Park, H.; Cheng, J.; Mader, B. T.; Hoffmann, M. R. Treatment technologies for aqueous perfluorooctanesulfonate (PFOS) and perfluorooctanoate (PFOA). *Front. Environ. Sci. Eng. China* **2009**, *3*, 129−151.
(51) Schuchmann, M. N.; Zegota, H.; von Sonntag, C. Acetate peroxyl radicals, $\cdot O_2CH_2CO_2^-$: A study on the γ-radiolysis and pulse radiolysis of acetate in oxygenated aqueous solutions. *Z. Naturforsch., B: J. Chem. Sci.* **1985**, *40*, 215−221.
(52) Kutsuna, S.; Hori, H. Rate constants for aqueous-phase reactions of SO_4^- with $C_2F_5C(O)O^-$ and $C_3F_7C(O)O^-$ at 298 K. *Int. J. Chem. Kinet.* **2007**, *39*, 276−288.
(53) Ervens, B.; George, C.; Williams, J.; Buxton, G.; Salmon, G.; Bydder, M.; Wilkinson, F.; Dentener, F.; Mirabel, P.; Wolke, R. CAPRAM 2.4 (MODAC mechanism): An extended and condensed tropospheric aqueous phase mechanism and its application. *J. Geophys. Res.* **2003**, *108*, 4426.
(54) Bentel, M. J.; Yu, Y.; Xu, L.; Kwon, H.; Li, Z.; Wong, B. M.; Men, Y.; Liu, J. Degradation of perfluoroalkyl ether carboxylic acids with hydrated electrons: Structure-reactivity relationships and environmental implications. *Environ. Sci. Technol.* **2020**, *54*, 2489−2499.
(55) Martin, D.; Munoz, G.; Mejia-Avendaćo, S.; Duy, S. V.; Yao, Y.; Volchek, K.; Brown, C. E.; Liu, J.; Sauvé, S. Zwitterionic, cationic, and anionic perfluoroalkyl and polyfluoroalkyl substances integrated into total oxidizable precursor assay of contaminated groundwater. *Talanta* **2019**, *195*, 533−542.
(56) Giessing, A. M.; Feilberg, A.; Møgelberg, T. E.; Sehested, J.; Bilde, M.; Wallington, T. J.; Nielsen, O. J. Atmospheric chemistry of HFC-227ca: Spectrokinetic investigation of the $CF_3CF_2CF_2O_2$

https://doi.org/10.1021/acs.est.1c00353
Environ. Sci. Technol. XXXX, XXX, XXX−XXX

radical, its reactions with NO and NO_2, and the atmospheric fate of the $CF_3CF_2CF_2O$ radical. *J. Phys. Chem.* **1996**, *100*, 6572−6579.
(57) Lin, H.; Niu, J.; Xu, J.; Huang, H.; Li, D.; Yue, Z.; Feng, C. Highly efficient and mild electrochemical mineralization of long-chain perfluorocarboxylic acids (C_9-C_{10}) by Ti/SnO_2-Sb-Ce, Ti/SnO_2-Sb/Ce-PbO_2, and Ti/BDD electrodes. *Environ. Sci. Technol.* **2013**, *47*, 13039−13046.
(58) Lutze, H. V.; Brekenfeld, J.; Naumov, S.; von Sonntag, C.; Schmidt, T. C. Degradation of perfluorinated compounds by sulfate radicals: New mechanistic aspects and economical considerations. *Water Res.* **2018**, *129*, 509−519.
(59) Bao, Y.; Deng, S.; Cagnetta, G.; Huang, J.; Yu, G. Role of hydrogenated moiety in redox treatability of 6:2 fluorotelomer sulfonic acid in chrome mist suppressant solution. *J. Hazard. Mater.* **2021**, *408*, 124875.
(60) Gu, Y.; Dong, W.; Luo, C.; Liu, T. Efficient reductive decomposition of perfluorooctanesulfonate in a high photon flux UV/Sulfite system. *Environ. Sci. Technol.* **2016**, *50*, 10554−10561.
(61) Vaughan, P. P.; Blough, N. V. Photochemical formation of hydroxyl radical by constituents of natural waters. *Environ. Sci. Technol.* **1998**, *32*, 2947−2953.
(62) Zepp, R. G.; Braun, A. M.; Hoigne, J.; Leenheer, J. A. Photoproduction of hydrated electrons from natural organic solutes in aquatic environments. *Environ. Sci. Technol.* **1987**, *21*, 485−490.
(63) Thomas-Smith, T. E.; Blough, N. V. Photoproduction of hydrated electron from constituents of natural waters. *Environ. Sci. Technol.* **2001**, *35*, 2721−2726.

https://doi.org/10.1021/acs.est.1c00353
Environ. Sci. Technol. XXXX, XXX, XXX−XXX